Journal of the European Ceramic Society **18** (1998) 417–427

PII: S0955-2219(97)00128-3
0955-2219/98/$19.00 + 0.00

Thermal Stability of Calcium α-sialon Ceramics

C. L. Hewett,[a] Y.-B. Cheng,[a]* B. C. Muddle[a] and M. B. Trigg[b]

[a]Department of Materials Engineering, Monash University, Wellington Road, Clayton, Victoria, 3168, Australia
[b]Commonwealth Science and Industrial Research Organisation (CSIRO), Division of Materials Science and Technology, Locked Bag 33, Rosebank MDC, Clayton, Victoria, 3169, Australia

(Received 12 May 1997; accepted 16 June 1997)

Abstract

The lack of thermal stability of some rare earth α-SiAlON phases has recently raised serious doubts concerning the high temperature behaviour of such materials. As information on the Ca–SiAlON system is minimal this work investigates the thermal stability behaviour of Ca α-SiAlON (α′). Compositions near the α′ plane in the Ca–Si–Al–O–N system were prepared by hot-pressing. These materials were subsequently heat treated at temperatures between 1100 and 1500°C for 24 h and for an extended duration, 200 h, at 1450°C. The addition of glass prior to hot-pressing to various compositions enabled the investigation of its effect on the initial phase assemblage and the thermal stability behaviour. It was found that neither the excess glass nor the heat treatment devitrification products, destabilised the Ca α′ phase. The presence of β′ grains appeared to facilitate the transformation behaviour of the Ca α′, however a single crystalline phase Ca α′ with a high value of m was thermally stable under extended heat treatment at 1450°C. © 1998 Elsevier Science Limited.

1 Introduction

The SiAlONs are structural ceramics developed for potential applications at elevated temperatures. The lack of thermal stability of some α-SiAlON (α') phases containing rare earth elements has, however, recently raised serious doubt concerning the high temperature performance of such materials. In studies involving post-sintering heat treatment of such SiAlONs, significant transformation from α' to β' has been observed at temperatures between 1100 and 1500°C.[1] The extent of the $\alpha' \rightarrow \beta'$ transformation increases with increasing temperature and duration of the heat treatment. Both α- and β-SiAlON have similar hexagonal crystal structures distinguished on the basis of differences in the stacking of the (Si,Al)$(O,N)_4$ tetrahedra. The formula for α-SiAlON is:

$$M_x^{v+} Si_{12-(m+n)} Al_{m+n} O_n N_{16-n} \quad (1)$$

where $x = m/v < 2$ and v is the valency of the stabilising cation, M, and for β-SiAlON (β') is:

$$Si_{6-z} Al_z O_z N_{8-z} \quad (2)$$

where $0 < z < 4{\cdot}2$ at 1750°C.[2] In contrast to the β' structure, in which long continuous open channels are formed parallel to the c-axis, the stacking of the α' structure creates large interstices occupied by the stabilising cation M. The transition from α' to β' requires long range diffusion of the cation species and significant lattice rearrangement, and is considered likely to be chemically controlled.[3] The mechanism of this transformation has recently become the subject of intense research, with various theories being proposed to explain the existence and extent of the α' to β' transition.

Initial focus on the factors influencing α' stability concerned the effective radius of the cation stabilising the α' structure,[3,4] with suggestions that a smaller stabilising cation would be more mobile and thus render the α' structure less stable. However, recent experimental evidence has shown that cation size and solubility alone cannot account for the intrinsic stability of the α' phase, and four additional factors have emerged as having potential importance:

1. the range of thermodynamic stability of α' and its variation with temperature,[1]
2. the fraction of cation, M, incorporated into the structure and the extent of corresponding (Al–O) and (Al–N) substitutions,[5,6]

*To whom correspondence should be addressed.

3. the presence of β' phase within the material as nucleation sites for the transformation,[7] and
4. the presence, volume and viscosity of an intergranular liquid/glassy phase,[8] and the stability of any devitrification products that result from post-sintering heat treatment.

In addition, significant variation in the response to heat treatment of α' stabilised by different cation indicates that the identity of the stabilising cation influences the thermal stability of the various M–SiAlON systems. Thus the extent to which the above four factors influence thermal behaviour may vary as the α' stabilising cation is changed.

Currently, the transformation is considered to have two distinct stages: (1) adjustment of the α' composition towards the region of α'/β' stability, which can be observed in a decrease in the m value with time at the heat treatment temperature, and (2) the subsequent decomposition of α' into β' and other phases.[9] Experimental results have shown that α' phases containing Nd and Sm (where the maximum cation solubility in the α' lattice occurs for $x = 0{\cdot}6$,[10] are among the α' structures that are most easily transformed to β', whereas the α' containing Yb (maximum solubility $x = 1{\cdot}0$)[10] is more stable over a wider range of temperatures.[5] If indeed α' stability increases with increasing cation solubility, then calcium α', which has the highest reported solubility for the cation ($x = 1{\cdot}83$),[11] might be expected to be one of the more stable α' ceramics. However, if the presence of intergranular liquid phase, or unstable glassy phase, destabilises the α' solid solution, then the calcium α' system might be expected to be one of the least stable, since the oxynitride glasses containing Ca have particularly low melting points.[12] The Ca–SiAlON system is thus an interesting one in which to evaluate those factors controlling the thermal stability of α' phases.

2 Experimental procedures

Samples with the nominal compositions listed in Table 1 were prepared from powder mixtures of Si_3N_4 (HCST LC10), AlN (HCST grade C), $CaCO_3$ (Ajax) and Al_2O_3 (Alcoa A16SG), ball milled using Si_3N_4 media in isopropanol. The anorthite ($CaO{\cdot}Al_2O_3{\cdot}2SiO_2$) and gehlenite ($2CaO{\cdot}Al_2O_3{\cdot}SiO_2$) glasses included in samples 2, 5 and 6 were prepared independently by heating to 1600°C for 1 h and water quenching to room temperature. The crushed glass was then added to the powder mixtures prior to milling. The slurries were pan dried and pressed uniaxially into pellets, cold isostatically pressed to 150 MPa, and calcined at 800°C for 1 h in a nitrogen atmosphere. Densification was carried out in a hot-press at temperatures between 1600 and 1800°C for 1 h at a pressure of 35 MPa in graphite dies and a nitrogen atmosphere. The sintered samples were then heat-treated at temperatures between 1100°C and 1500°C for 24 and 200 h in an alumina tube furnace under a nitrogen atmosphere. Bulk densities of the samples were determined after boiling for 2 h in distilled water followed by application of water immersion techniques. Phase identification both before and after post-sintering heat treatment was carried out using a Rigaku Geigerflex diffractometer with Ni-filtered Cu K_α radiation. The weight ratio of α' to β' phase was calculated using a method developed by Liddell.[13] Lattice parameter determinations were carried out using a Hägg–Güinier camera and the program CELSIZ.[14] From the a and c lattice parameters, the values of m for the α-SiAlONs [eqn (1)] were calculated using the following pair of equations:[15]

$$\begin{aligned} a(A) &= 7{\cdot}749 + 0{\cdot}0023n + 0{\cdot}0673m \\ c(A) &= 5{\cdot}632 - 0{\cdot}0054n + 0{\cdot}0550m \end{aligned} \tag{3}$$

The values of z for the β' were calculated according to the following:[16]

$$\begin{aligned} a(A) &= 7{\cdot}603 + 0{\cdot}0297z \\ c(A) &= 2{\cdot}907 + 0{\cdot}0255z \end{aligned} \tag{4}$$

Polished, as-sintered samples were etched in molten NaOH, carbon coated to prevent charging and observed using a JEOL JSM-840A scanning electron microscope (SEM).

3 Results

The nominal compositions and corresponding lattice parameters of all as-sintered samples prior to heat treatment are listed in Table 1, which also includes measurements of the ratio of the α' to β' phases in the as-fired samples, as determined by X-ray diffraction (XRD). Figure 1 shows the three-dimensional Jänecke prism for the Ca–Si–Al–O–N system in which there exists a triangular plane section that contains the α' phase region. The three base sample compositions employed are depicted in a two-dimensional schematic representation around the α' phase region in Fig. 2.

The sample compositions selected were designed to give α' solid solutions in various phase regions and different chemical environments, including the presence of pre-existing β' phase and/or

Table 1. The initial composition, $\alpha':\beta'$ ratios, lattice parameters and associated m and z values for the α' and β', respectively, of the six materials prior to heat treatment. The α lattice parameters, and associated values of m for samples heat treated at 1450°C for 24 h and 200 h

Sample		*Sample 1 (nominally m = 2, n = 2)*	*Sample 2 (composition 1 plus 15 wt% anorthite glass)*	*Sample 3 (nominally m = 1, n = 2)*	*Sample 4 (composition 3 plus 30 wt% Si_3N_4)*	*Sample 5 (composition 4 plus 15 wt% anorthite glass)*	*Sample 6 (composition 4 plus 15 wt% gehlenite glass)*
$\alpha':\beta'$ ratio prior to heat treatment		100 : 0	100 : 0	93 : 7	64 : 36	10 : 90	78 : 22
α' lattice parameters prior to heat treatment	*a*	7·8562(8)[a]	7·8382(6)	7·8172(4)	7·8012(4)	7·8055(17)	7·8085(5)
	c	5·7124(9)	5·7013(4)	5·6886(4)	5·6751(5)	5·6812(25)	5·6759(7)
	m[b]	1·6	1·3	1·1	0·8	0·9	0·9
β' lattice parameters prior to heat treatment	*a*	—	—	—	7·6272(7)	7·6319(8)	7·6246(19)
	c	—	—	—	2·9227(7)	2·9247(8)	2·9190(13)
	z[c]	—	—	—	0·7	0·8	0·6
α' lattice parameters after heat treatment at 1450°C for 24 h	*a*	7·8520(4)	7·8348(5)	7·8155(5)	7·8009(4)	7·8069(12)	7·8055(7)
	c	5·7127(3)	5·7010(4)	5·6880(5)	5·6741(5)	5·6785(17)	5·6746(10)
	m	1·51	1·27	1·00	0·77	0·86	0·82
α' lattice parameters after heat treatment at 1450°C for 200 h	*a*	7·8461(4)	7·8302(5)	—	—	—	—
	c	5·7105(3)	5·6993(4)	—	—	—	—
	m	1·44	1·21	—	—	—	—

[a]The standard deviation of the last decimal place in the lattice parameter is given in the parentheses.
[b]The m value from eqn (1) calculated using the pair of eqn (3).
[c]The z value from eqn (2) calculated using the pair of eqn (4).

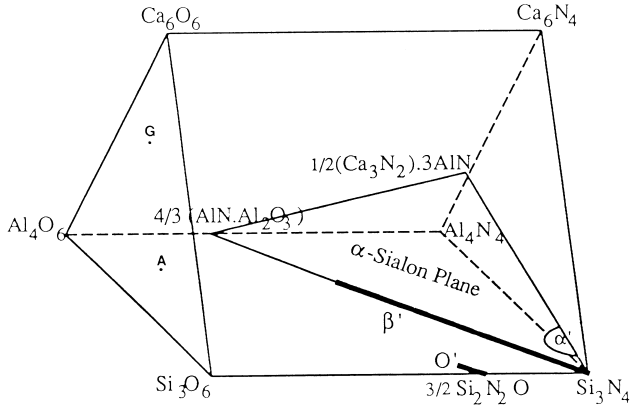

Fig. 1. The Jänecke prism for the calcium SiAlON system, showing the position of the α-SiAlON plane. Note: G and A represent gehlenite and anorthite compositions, respectively.

oxide-based amorphous (liquid) phases of varying composition. Sample 1 has the same nominal composition as the material described in earlier work[17] to comprise exclusively α', with a very small fraction (< 5wt%) of residual glassy phase. The addition to composition 1 of 15 wt% glass, rich in silica and with a composition of anorthite, had the effect of moving the overall composition off the α' plane to produce sample 2, containing α', a significant fraction of glass, and two minor phases, calcium aluminate and anorthite. These minor phases are oxide based and may have formed during cooling, quenching the material from the fabrication temperature may prevent any devitrification of the glassy phase.

To investigate the effect of the presence of pre-existing β' phase in a predominantly α' material, sample 3 was designed to lie just outside the single phase α' region and in the $\alpha'+\beta'$ two phase region. The addition of 30 wt% Si_3N_4 to composition 3, to create sample 4, shifted the composition towards the Si_3N_4 corner and significantly increased the fraction of pre-existing β' phase in the as-fired sample. Samples 5 and 6 were both based on the composition 4. The additions of 15 wt% anorthite glass and 15 wt% calcia-rich gehlenite glass, to form samples 5 and 6, respectively, produced materials that contained both α' and β' phases, with an amorphous grain boundary phases of different compositions.

Observation of the microstructures of the as-fired samples in the scanning electron microscope (SEM) revealed significant differences. Figure 3 shows that the addition of glass had a dramatic effect on the microstructure leading to a coarsening of the grain size. The elongated nature of β' grains allows them to be easily distinguished from the more equiaxed α'. Figure 3(a) is the microstructure observed for the single phase α' (sample 1), while Fig. 3(b) reveals sample 2, composed of α', glass and minor oxide phases, to have a coarser-grained microstructure than that observed for sample 1. After etching in molten NaOH the increase in the fraction of glassy grain boundary phase in sample 2 can be readily distinguished qualitatively.

Figure 3(c)–(e) depicts samples 4, 5 and 6, respectively. Sample 4 is an α'/β' composite with an $\alpha':\beta'$ ratio of 64:36, while samples 5 and 6 [Fig. 3(d) and (e)] shows the effect of the addition of anorthite and gehlenite glass, respectively. Sample 4

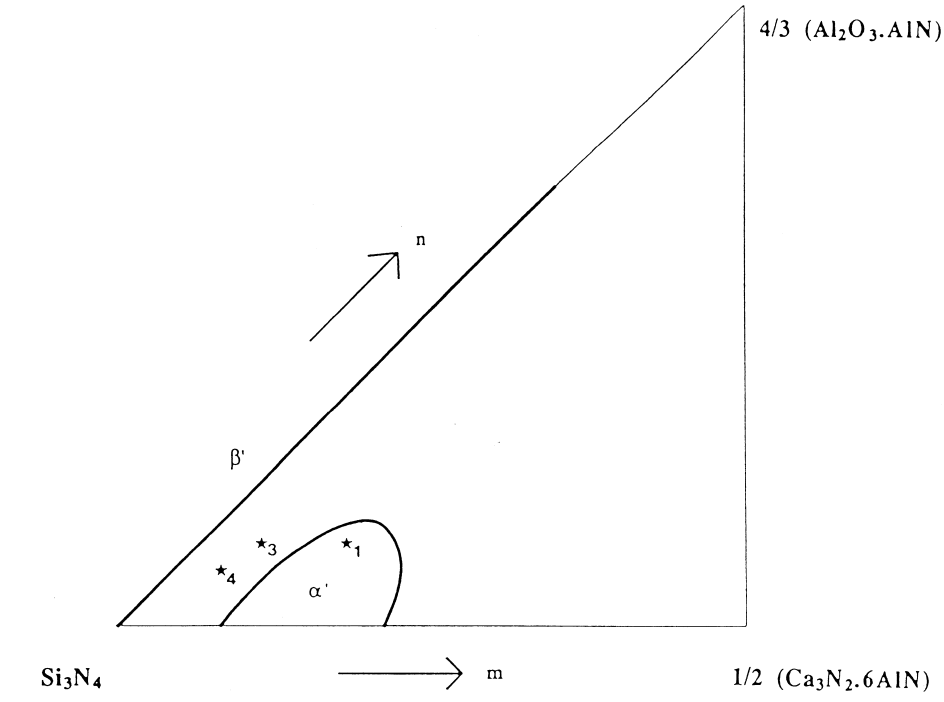

Fig. 2. The 2D α' plane for the calcium SiAlON system, indicating the position of the three base compositions, samples 1, 3 and 4.

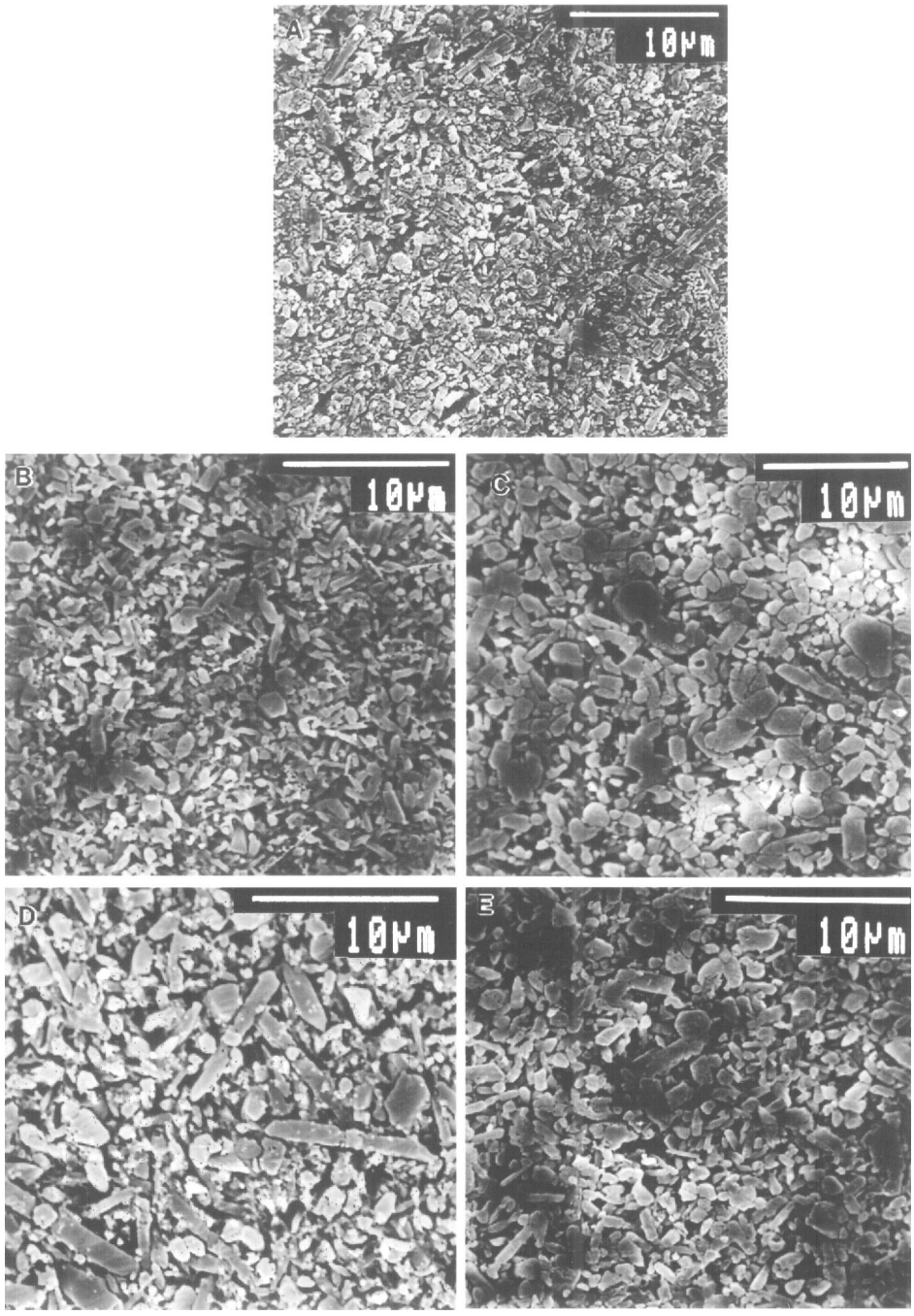

Fig. 3. SEM micrographs of samples 1, 2, 4, 5 and 6 (a)–(e), respectively.

(α':β' = 64:36) contained a mixed microstructure of equiaxed and elongated grains [Fig. 3(c)] and the grain size was generally much coarser than that observed for both samples 1 and 2. Scanning electron microscopy of sample 5 (α':β' = 10:90) [Fig. 3(d)] revealed coarser, more elongated grains of high aspect ratio (4:1 to upwards of 10:1) compared to Fig. 3(c). The addition of anorthite glass appears to have reduced the constraints on grain growth during precipitation from the liquid phase, resulting in characteristic grains with a high aspect ratio. In contrast, the addition of gehlenite glass to produce sample 6 resulted in a more equiaxed microstructure and this can be directly related to the phase changes induced by the glass addition, that is, the compositional equilibrium shift from an α':β' ratio of 64:36 in sample 4 to the 78:22 observed in sample 6. The significant variation observed in the microstructures resulting from the addition of the two different glass compositions to the same initial powders, fabricated under similar conditions, implies that the resultant ratio between α' and β' phases is dependent on the composition of the oxynitride liquid that forms during sintering and prior to SiAlON precipitation. The m value is similar for both samples 5 and 6 (Fig. 1), implying that the level of Ca^{2+} cation solubility within the α' lattice is comparable. The similar values for m imply that the higher calcium content in the gehlenite-containing sample 6 enables a higher

proportion of α' grains to be stabilised, thereby resulting in more equiaxed grains.

Changes in the lattice parameters for the α' and β' phases represent compositional variation in the solid solutions. The Al–N bond is significantly larger (0·187 nm)[11] than the Si–N bond, and Al–N substitution for Si–N creates a negative valence difference, requiring an increased cation concentration to balance charge over the unit cell. The introduction of Al–N bonds for Si–N bonds within the α' lattice results in an expansion of the unit cell and requires a higher proportion of Ca^{2+} to stabilise the structure. The Si–N and Al–O bond lengths are almost identical, at 0·174 nm and 0·175 nm, respectively,[11] and the net valency difference arising within α-SiAlON from Al–O substitution alone is effectively zero. From the measured lattice parameters, Table 1, it is noted that the α' phase of sample 1 has the largest unit cell suggesting that this α' structure incorporates the largest fraction of Ca^{2+} and has the most extensive substitution of Al–N bonds for Si–N bonds. The addition of 15 wt% anorthite glass to composition 1 produced a material with a single nitrogen rich crystalline phase, Ca α', but the composition change thus imposed on the α' in sample 2 is reflected in a reduction in the unit cell dimensions (Table 1). This reduction in the α' lattice parameters implies an increase in the number of oxygen bonds in the structure, and thus a decrease in the calcium content of the α'.

The smallest α' lattice parameters were observed in samples 4–6, where all three materials contained a large fraction of β' with a nominal z value between 0·6 and 0·8. The coexistence of α' and β' in these three samples indicates a phase equilibrium on the tie line between the α' and the β' regions and that the composition of the α' phase would be at the boundary of the single phase α' field, close to the Si_3N_4 corner. At this boundary, the value of m for the α' [eqn (1)] is low, corresponding to a reduced substitution of Al–N bonds and a lower concentration of Ca^{2+} in the α' lattice. The combined effect is to reduce the size of the unit cell.

The lattice parameters of the α' and β' phases and the corresponding values of m and z of all samples prior to heat treatment are presented in Table 1. Also included are the α' lattice parameters of the samples heat treated at 1450°C for 24 and 200 h. Both samples 1 and 2 exhibit substantial stability at 1450°C and show only small decreases in the α':β' ratio after 200 h exposure.

The weight ratios of α' to β' phase for all seven samples prior to heat treatment are included in Table 1, while Table 2 shows the α':β' ratios and the devitrification products in each sample resulting from heat treatment at selected temperatures. Crystalline grain boundary phases were detected after heat treatment for all samples; however, the temperature of formation and the identity of the phases produced varied from sample to sample. Gehlenite was the most prevalent product in samples 1, 2, 4, 5, and 6 and was observed to be stable in the temperature range 1200 to 1500°C. The S-phase ($CaO{\cdot}1{\cdot}33Al_2O_3{\cdot}0{\cdot}67Si_2N_2O$)[18] was also identified as a devitrification product in samples 2 and 5, and very small fractions of an unidentified phase were detected in samples 3 and 5 heat treated between 1100 and 1500°C. Gehlenite is identified by three clearly distinguishable Bragg diffraction peaks, from the planes (111), (201) and (211), due to significant overlap of the remaining peaks with those of both the α' and β' phases, and therefore the determination of the extent, if any, of the gehlenite solid solution with nitrogen is not pursued here. Figure 4 depicts the XRD traces of sample 5 before and after heat treatment at 1300°C for 24 h and 1500°C for 24 h, respectively. The variation in devitrification products with temperature is clearly identified, as S-phase and gehlenite were observed after heat treatment at 1300°C for 24 h. However after heat treatment at 1500°C for 24 h, the only devitrification product detected was gehlenite. Given that the emphasis of the present paper is the thermal stability of the Ca α' phase, further analysis of the devitrification products will not be pursued in detail here, although the work is continuing.

4 Discussion

Sample 1 contained almost exclusively crystalline α' phase, with a limited amount of glass at the grain boundaries.[17] This composition is located within the α' phase region and the α' structure resists decomposition into β' at temperatures up to 1500°C. However, when the length of the post-sintering isothermal heat treatment was increased to 200 h at 1450°C, the presence of ~3 wt% β was detected using XRD, indicating that the material would eventually undergo at least partial transformation from α' to β'. Single phase Ca rich α' is nonetheless substantially more stable than the rare earth stabilised α' systems. In the Sm α' system, for example, an essentially single phase material with a value $x = 0{\cdot}39$ was observed to begin transformation to β' within 24 h at 1450°C,[19] while that same initial transformation required 200 h at 1450°C in the Ca α' system.

In other rare earth α' systems, the addition of glass to an initially α' composition may result in the formation of a two-phase α'/β', material and during subsequent heat treatment the $\alpha' \rightarrow \beta'$

Table 2. Phase analysis of the post-sintering heat treated samples, indicating the α' to β' ratio numerically and the intensity of the other phases present by tr = trace, w = weak, m = medium s = strong and v = very

Heat treatment temperature	*Sample 1 (m = 2, n = 2)*	*Sample 2 (composition 1 + anorthite glass)*	*Sample 3 (m = 1, n = 2)*	*Sample 4 (composition 3 + 30 wt% Si_3N_4)*	*Sample 5 (composition 4 + 15 wt% anorthite glass)*	*Sample 6 (composition 4 + 15 wt% gehlenite glass)*
Initial phases present	α'(100:0)	α'(100:0), CA(w), A(mw)	α'(93), β'(7)	α'(64),β'(36)	α'(10),β'(90)	α'(78), β'(22), G(w)
HT 1100°C 24 h^{-1}	α'(100:0)	α'(100:0), CA(w), G(mw)	α'(93), β'(7)	α'(64), β'(36)	*	*
HT 1200°C 24 h^{-1}	α'(100:0)	α'(100:0), CA(w), G(mw), S(w)	α'(93), β'(7)	α'(63), β'(37), G(tr)	α'(11),β'(89), G(mw), S(mw), ?[2](2)	α'(83), β'(17),G(mw)
HT 1300°C 24 h^{-1}	α' (100:0), G(vw)	α' (100:0), G(mw), S(mw)	α'(93), β'(7), ?(vw)	α'(61), β'(39), G(vw)	α'(l2), β'(88), G(mw),S(mw), [2](w)	α'(82), β'(18) G(mw)
HT 1400°C 24 h^{-1}	α' (100:0), G(vw)	α'(100:0), G(mw), S(mw)	α'(93), β'(7), ?(tr)	α'(60), β'(40), G(tr)	α'(11), β'(89), G(mw)	α'(82), β'(18), G(mw)
HT 1450°C 24 h^{-1}	α' (100:0), G(vw)	α'(100:0) G(ms), S′(w)	α'(93), β'(7)	α'55), β'(45), G(tr)	α'(9), β'(91)	α'(77), β'(23), G(mw)
HT 1500°C 24 h^{-1}	α' (100:0), G(wv)	α'(100:0), G(m), S′(w)	α'(93), β'(7)	α'(62), β'(38), G(tr), ?(w)	α'(l2), β'(88), G(w), ?[2](w)	α'(83), β'(17), G(m)
HT 1450°C 200 h^{-1}	α'(97), β'(3) G(tr)	α'(93), β'(3), G(tr)	α'(52), β'(48)	α'(24), β'(76), G(vw)	β'(100), ?[2](w)	α'(36), β'(64), ?[3](m)

α'JCPDS33–261;β'JCPDS36–1333; G (gehlenite) JCPDS35–755; CA (calcium aluminate) JCPDS33–251; A (anorthite) JCPDS12–301; S (s-phase $CaO{\cdot}1{\cdot}33Al_2O_3{\cdot}0{\cdot}67S_2N_2O$) JCPDS43–281; ?x are unknown phases.

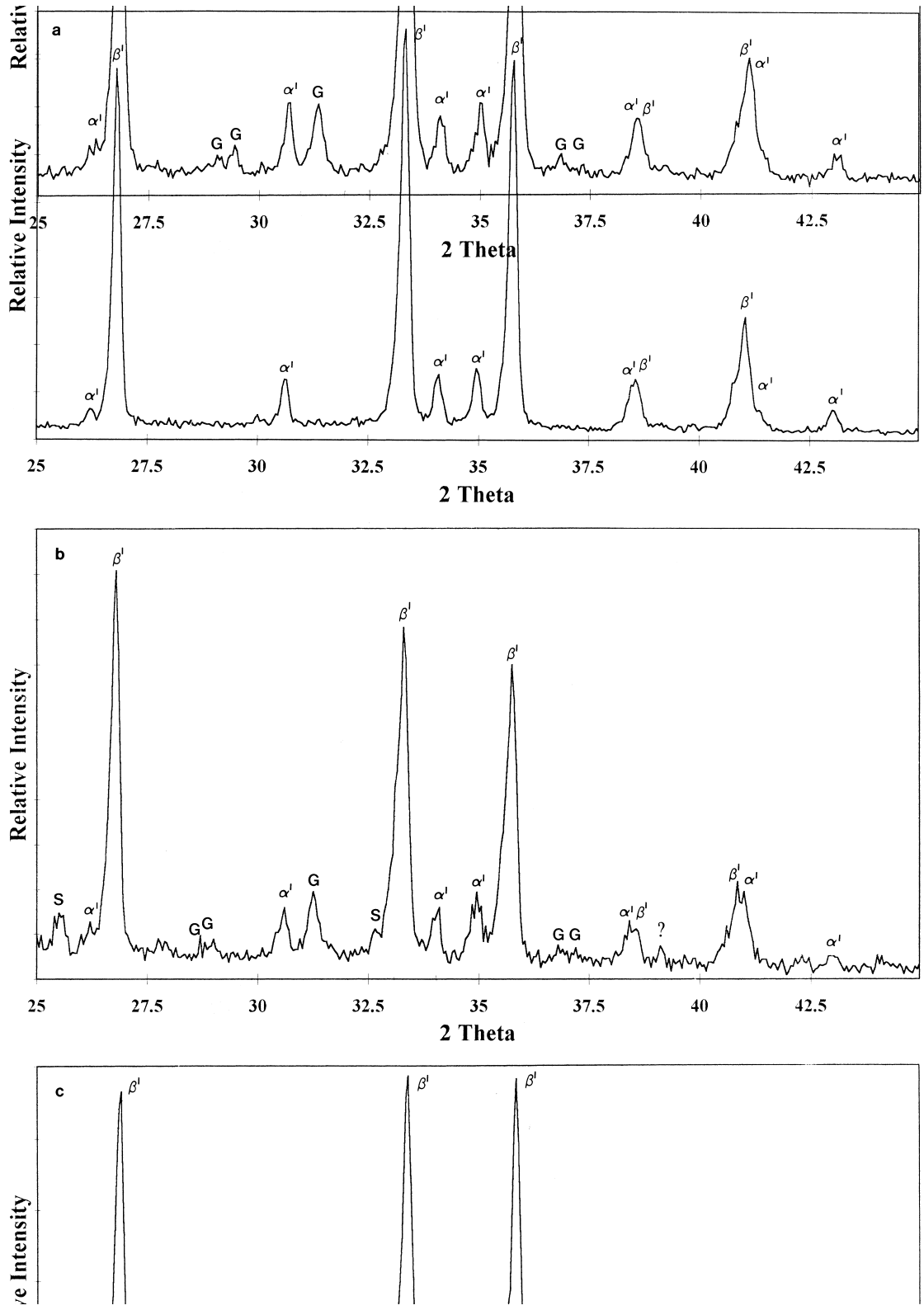

Fig. 4. X-ray diffraction traces of sample 5, (a) prior to and (b) post heat treatment at 1300°C and (c) at 1500°C for 24 h. Note: G = gehlenite, S = S–phase, ? = unidentified phase.

transformation may be facilitated.[20] Mandal *et al.*[21] have proposed that the presence of large volumes of low viscosity grain boundary glassy/liquid phase surrounding the α' and β' grains facilitates the initial transformation by allowing atom diffusion at the heat treatment temperatures. The composition of the oxynitride liquid may affect the rate of the transformation from α' to β'; it has been suggested that a more oxide-rich liquid will have a lower viscosity and increase significantly the rate of the α' to β' transformation.[21] The composition and the nature of the glassy phase in the α' system is seen to be critical to the stability of α' phases.

Results of the present investigation are in contrast with rare earth α' systems examined by McKinnon *et al.*[20] and Mandal *et al.*[21] In the calcium system the addition of 15 wt% anorthite glass in sample 2 was not observed to introduce any detectable β' phase into the as-sintered material, nor did it obviously degrade the thermal stability of the α' phase. This result is, in part, the consequence of the more extensive region of α' stability in the Ca–SiAlON system compared with rare earth systems, as the additional oxide glass has not displaced the sample composition into the α'/β' two phase field. In addition, α' compositions close to the Al–N rich edge of the phase region (implied by the larger unit cell parameters, and m values of sample 1 and 2 compared with samples 3–6, Table 1) are very stable at elevated temperatures. Heat treatment for extended periods of time (200 h at 1450°C) revealed that the transformation from α' to β' does proceed in sample 2 to a similar extent to that detected in sample 1, and that, the rate of transformation is not obviously affected by the larger fraction of amorphous phase present in sample 2.

The fraction of Al–O and Al–N bonds replaced within the α lattice and, consequently, the concentration of cation species required to balance valencies may also affect the thermal stability of α'. In materials nearing the lower cation solubility limit, the α' is regarded as likely to be less stable and the $\alpha' \rightarrow \beta'$ transformation considered more readily able to proceed.[5] This apparent correlation between the cell dimensions of the α' phase and the potential for $\alpha' \rightarrow \beta'$ transformation implies that those α' structures with large unit cells (e.g. $a > 7{\cdot}83$ Å and $c > 5{\cdot}70$Å in the present system) will be more stable than those having a relatively small unit cell. This would suggest that those α' compositions nearer to the $1/2(Ca_3N_2{\cdot}6AlN)$-rich boundary of the phase field might demonstrate higher thermal stability.

The cell dimensions and the values of m for the α' phases in samples 1 and 2 decreased continuously during prolonged heat treatment at 1450°C (Table 1). It is suggested that both diffusion of Ca^{2+} as well as Al^{3+} and N^{3-} occurs within the α' structure during the heat treatment process. However, the precise mechanism for these changes remains unclear at this stage. These changes in the structure and composition of the α' are associated with the appearance of a small fraction of β' in these two samples after 200 h at 1450°C and they may thus signal the eventual destabilisation of the α' phase.

As a result of the dual-phase (α'/β') nature observed for sample 3, the α' composition is expected to be defined at the boundary of the α' phase zone. It correspondingly exhibits a relatively small unit cell and m value, Table 1. However, this α' structure proved to be thermally stable for up to 24 h at all temperatures despite the existence of β' grains to provide potential nucleation sites for the transformation. The initial $\alpha':\beta'$ ratio of sample 3 was 93:7, but upon increasing the duration of heat treatment to 100 h then 200 h at 1450°C, there was evidence of transformation and the $\alpha':\beta'$ ratio decreased to 85:15 and 52:48, respectively. This suggests that the α' with the smaller lattice dimensions in sample 3 is less stable than the α' with the larger unit cell in sample 1, which required 200 h at 1450°C before detectable transformation. This is in agreement with the work of Shen *et al.* in the ytterbium α' system.[5] It has been suggested[9] that a single phase α' material subjected to heat treatment undergoes compositional adjustment over time, with the composition moving continuously towards the boundary between the single phase α' region and the α'/β' region. Once at this boundary, the α' is unstable and decomposition may take place. Another factor contributing to the change in the ratio of α' to β' may be the reduction in size of the single phase α' forming region with decreasing temperature that is observed in other rare earth stabilised systems.[1] The Ca α' system, however, is stable at the heat treatment temperatures for extended durations and this may indicate that in the Ca α' system, variation in the size of the α' phase region with temperature is small. The thermal stability of sample 1 coupled with the transformation behaviour of sample 3, whose initial composition is at the $\alpha':\alpha'/\beta'$ boundary, supports the notion of an adjustment in the composition of the α' towards the α'/β' region and a reduction in the thermal stability of the resulting α'.

Zhao and Cheng[7,22] have suggested that the presence of β' grains within an α'-based material may facilitate the progress of the $\alpha' \rightarrow \beta'$ transformation. This proposal is supported by the observations in the Ca α' system (Table 2). Sample 1

(100% α') and sample 3 ($\alpha':\beta' = 93:7$) show significantly different degrees of transformation after heat treatment at 1450°C for 200 h. It is suggested that sample 1 requires nucleation of new β' grains for the transformation to proceed and thus the transition from α' to β' is still in the initial stages. In sample 3 however, the transformation may proceed via growth of the pre-existing β' grains or the β' grains may provide preferred heterogeneous nucleation sites for decomposition. With reduced barriers to nucleation and growth the material transforms at a greater rate, with a resultant ratio of $\alpha':\beta'$ of 52:48 after 200 h. In addition, it is important to recognise that the α' phase field may shrink with decreasing temperature from 1700 to 1450°C which would imply a greater fraction of β' after heat treatment at 1450°C, as a result of the required adjustments in the compositions of the phases.

It is indicated from the above results that the thermal stability of an α' phase is governed by the intrinsic characteristics of the phase, namely its composition and the identity of the stabilising cation. Extrinsic features of the microstructure, such as the presence of grain boundary glass and/or pre-existing β' phase may only act to assist the α'/β' transformation.

The nature of the phases that result from the devitrification of the amorphous grain boundary phase during post-sintering heat treatment may also affect the thermal stability of the α'. The formation of a cation-rich grain boundary phase, that arises during the devitrification of the amorphous phase, will result in a partition of a significant portion of the cation into the glass and may compete for the remaining cation within the α'. The melilite solid solutions formed in the Sm α' system, for example, consume the Sm^{3+} cations and this is thought to be a factor in the destabilisation of Sm α'.[6] Therefore the higher thermal stability observed for the Ca α' phases may also be a result of the lack of any stable nitrogen rich devitrification phases (other than β') in the Ca–SiAlON system. The devitrification of the grain boundary glass into phases such as gehlenite and S-phase during post sintering heat treatment in the Ca–SiAlON system, while the $\alpha':\beta'$ ratio remains constant (e.g. sample 5 heat treated at 1300°C for 24 h), suggests that these phases do not destabilise the Ca α' in order to compete for increased fractions of the Ca^{2+} cation. Thus the Ca α' solid solutions appear generally more stable than those rare earth α' systems studied to date.

Sample 4 had 30 wt% additional Si_3N_4 compared to sample 3, which displaces the composition further from the $1/2(Ca_3N2{\cdot}6AlN)$–$4/3$ ($Al_2O_3{\cdot}AlN$) edge. As a result, more β' was formed and the α' phase had a smaller unit cell than that in sample 3. Samples 5 and 6 also contained β' and had smaller lattice parameters and corresponding m values than samples 1, 2 or 3. After heat treatment at all experimental temperatures for 24 h, the α' to β' ratios of these samples (5 and 6) had not changed within experimental error and the fluctuations observed are too small to offer conclusive evidence of the transformation. However, increasing the duration of heat treatment to 200 h at 1450°C led to destabilisation of the α' and sample 5 transformed completely to β', while significant transformation was observed in sample 6.

Comparing the Ca α' system with those that are rare earth-stabilised, the amount of α' to β' transformation recorded at 1450°C for 24 h in the Sm system (initial $\alpha':\beta'$ ratio of 40:60, post heat treatment ratio 0:100) and the Yb system (initial $\alpha':\beta'$ ratio of 80:20, post heat treatment ratio 10:90),[4] the thermal stability of the Ca α' system has been found to be superior for the shorter duration heat treatments, irrespective of the presence of large volumes of glassy phase or the pre-existence of β' grains. Single phase Ca α' also exhibits excellent thermal stability under extended heat treatments.

5 Conclusions

The Ca α-SiAlON solid solutions investigated in this work have shown thermal stability superior to rare earth-stabilised (e.g. Nd and Sm) α' phases. Comparison of the thermal stability of samples containing single phase α' (sample 1) and single phase α' with excess glass (sample 2) after 200 h at 1450°C indicates that the presence of large fractions of glassy phase in the material has little effect on the initial rate of $\alpha' \rightarrow \beta'$ transformation in the Ca–SiAlON system. The presence of devitrification products in the Ca–SiAlON system does not destabilise the Ca α' during post-sintering heat treatments. The existence of β' grains in the as-sintered ceramic appears to affect the transformation behaviour of the material under heat treatment. However, a single phase α' material exhibits excellent thermal stability under extended post-sintering heat treatments.

The conclusions obtained in this work support the proposal that the α' to β' transformation is a two stage process; the composition of the α' phase during extended heat treatment is continually adjusted towards the α': α'/β' boundary, followed by the decomposition of the resultant α'. This suggests that an α' lattice with a high cation solubility will exhibit better thermal stability.

Acknowledgements

The authors acknowledge the research grant provided by the Australian Research Council to undertake this work. They also wish to thank Dr David Hay (CSIRO) for his guidance with the Güinier camera work.

References

1. Mandal, H., Thompson, D. P and Ekström, T., Reversible $\alpha \Longleftrightarrow \beta$ transformation in heat treated SiAlON ceramics. *Journal of the European Ceramic Society*, 1993, **12**, 421–429.
2. Jack, K. H., Review: SiAlONs and related nitrogen ceramics. *J. Mater. Sci.*, 1976, **11**, 1135–1158.
3. Thompson D. P., $\alpha \Longleftrightarrow \beta$ SiAlON transformation. In *Tailoring of Mechanical Properties of Si_3N_4 Ceramics,* ed. M. J. Hoffmann and G. Petzow. Kluwer Academic Press, Dordrecht, The Netherlands, 1994, pp. 125–136.
4. Mandal, H., Thompson, D. P. and Ekström, T., Optimisation of SiAlON ceramics by heat treatment. In *Third Euro-Ceramics*, Vol. 3, ed. P. Duran and J. F. Fernandez. Faenza Editrice Iberica, Spain, 1993, pp. 385–390.
5. Shen, Z., Ekström, T. and Nygren, M., Ytterbium stabilised α-SiAlON ceramics. *J. Phys. D: Appl. Phys.*, 1996, **29**, 893–904.
6. Shen, Z., Ekström, T. and Nygren, M., Reactions occurring in post sintering heat-treated α/β SiAlONs: on the thermal stability of α SiAlON. *Journal of the European Ceramic Society*, 1996, **16**, 873–883.
7. Zhao, R. and Cheng, Y.-B., Decomposition of α-SiAlON phase during post-sintering heat treatment. *Journal of the European Ceramic Society*, 1996, **15**, 1221.
8. Mandal, H. and Thompson, D. P., Mechanism for the $\alpha \Longleftrightarrow \beta$ SiAlON transformation. In *4th E. Cer. S. Conference Proceedings*, Vol 2, ed. C. Galassi. Editoriale Faenza Editrice Societa Cermaica Italiana, Gruppo, 1995, pp. 327–334.
9. Ekström, T., α-SiAlON and α/β-SiAlON composites: recent research. In *Engineering Ceramics '96: Higher Reliability Through Processing*, ed. G. N. Babini, M. Haviar and P. Sajgalik, Kluwer Academic Publications, Dordrecht, The Netherlands, 1997, pp. 147–167.
10. Huang, Z.-K., Tien, T.-Y. and Yen, T.-S., Subsolidus phase relationships in Si_3N_4–AlN–rare earth oxide systems. *J. Am. Ceram. Soc.*, 1986, **69**(10), C241–C242.
11. Jack, K. H., The characterisation of α-SiAlONs and the α–β relationship in SiAlONs and silicon nitrides. In *Progress in Nitrogen Ceramics*, ed. F. L. Riley. Matinus Nijhoff, Hague, The Netherlands, 1983, pp. 45–49.
12. Levin, E., Robbins, C. and McMurdie, H. (editors), Figure 630. In *Phase Diagrams for Ceramicists*, 1964, Am. Ceram. Soc.
13. Liddell, K., X-ray analysis of nitrogen ceramic phases. MSc. thesis, University of Newcastle upon Tyne, 1979.
14. Scott, H. J., CELSIZ program, CSIRO, Australia, 1986.
15. van Rutten, J. W. T., Hintzen, H. T. and Metselaar, R., Phase formation of Ca α-SiAlON by reaction sintering. *Journal of the European Ceramic Society*, 1996, **16**, 995–999.
16. Ekström, T., Käll, P. O., Nygren, M. and Olsson, P. O., Dense single phase β-SiAlON ceramics by glass encapsulated hot isostatic pressing. *J. Mater. Sci.*, 1989, **24**, 1853–1861.
17. Hewett, C. L., Cheng, Y.-B., Muddle, B. C. and Trigg, M. B., Preparation of fine grained calcium α-SiAlON. *J. Mater. Sci. Lett.*, 1994, **13**, 1612–1615.
18. Sun, W. Y., Yen, T. S. and Tien, T. Y., Subsolidus phase relationships in part of the system Si,Al,Ca/N,O. *Ceram. Int.*, 1988, **14**, 199–205.
19. Ekström, T., Shen, Z. and Falk, L., Duplex α–β SiAlON ceramics stabilised by dysprosium and samarium. *J. Am. Ceram. Soc.*, 1997, **80**(2), 301–312.
20. McKinnon, J., Cheng, Y.-B. and Trigg, M. B., Stability of α-SiAlON. In PacRim2 Conference Proceedings, July 1996, to be published.
21. Mandal, H., Camsucu, N. and Thompson D. P., Comparison of the effectiveness of rare earth sintering additives on the high temperature stability of α-SiAlON ceramics. *J. Mater. Sci*, 1995, **30**, 5901–5909.
22. Zhao, R., Cheng, Y.-B. and Drennan, J., Microstructural features of the α- to β-SiAlON phase transformation. *Journal of the European Ceramic Society*, 1996, **16**, 529–534.